Received: 23 February 2023 | Revised: 11 July 2023 | Accepted: 21 July 2023

DOI: 10.1002/jex2.106

RESEARCH ARTICLE

Survey of organ-derived small extracellular vesicles and particles (sEVPs) to identify selective protein markers in mouse serum

Kotb Abdelmohsen[1] | **Allison B. Herman**[1] | **Angelica E. Carr**[1] | **Charnae' A. Henry-Smith**[1] | **Martina Rossi**[1] | **Qiong Meng**[1] | **Jen-Hao Yang**[1] | **Dimitrios Tsitsipatis**[1] | **Alhassan Bangura**[1] | **Rachel Munk**[1] | **Jennifer L. Martindale**[1] | **Carlos J. Nogueras-Ortiz**[4] | **Jon Hao**[2] | **Yi Gong**[1] | **Yie Liu**[1] | **Chang-Yi Cui**[1] | **Lisa M. Hartnell**[3] | **Nathan L. Price**[3] | **Luigi Ferrucci**[3] | **Dimitrios Kapogiannis**[4] | **Rafael de Cabo**[3] | **Myriam Gorospe**[1]

[1]Laboratory of Genetics and Genomics, National Institute on Aging Intramural Research Program (NIA IRP), National Institutes of Health (NIH), Baltimore, Maryland, USA

[2]Poochon Scientific, Frederick, Maryland, USA

[3]Translational Gerontology Branch, NIA IRP, NIH, Baltimore, Maryland, USA

[4]Laboratory of Clinical Investigation, NIA IRP, NIH, Baltimore, Maryland, USA

Correspondence
Myriam Gorospe and Kotb Abdelmohsen, Laboratory of Genetics and Genomics, National Institute on Aging IRP, National Institutes of Health, 251 Bayview Blvd., Baltimore, MD 21224, USA.
Email: myriam-gorospe@nih.gov; abdelmohsenk@mail.nih.gov

Funding information
Myriam Gorospe, Grant/Award Number: Z01-AG000511; National Institute on Aging Intramural Research Program; National Institutes of Health

Abstract

Extracellular vesicles and particles (EVPs) are secreted by organs across the body into different circulatory systems, including the bloodstream, and reflect pathophysiologic conditions of the organ. However, the heterogeneity of EVPs in the blood makes it challenging to determine their organ of origin. We hypothesized that small (s)EVPs (<100 nm in diameter) in the bloodstream carry distinctive protein signatures associated with each originating organ, and we investigated this possibility by studying the proteomes of sEVPs produced by six major organs (brain, liver, lung, heart, kidney, and fat). We found that each organ contained distinctive sEVP proteins: 68 proteins were preferentially found in brain sEVPs, 194 in liver, 39 in lung, 15 in heart, 29 in kidney, and 33 in fat. Furthermore, we isolated sEVPs from blood and validated the presence of sEVP proteins associated with the brain (DPP6, SYT1, DNM1L), liver (FABPL, ARG1, ASGR1/2), lung (SFPTA), heart (CPT1B), kidney (SLC31), and fat (GDN). We further discovered altered levels of these proteins in serum sEVPs obtained from old mice compared to young mice. In sum, we have cataloged sEVP proteins that can serve as potential biomarkers for organ identification in serum and show differential expression with age.

KEYWORDS
aging, biofluids, biomarker, exosomes, organ-derived extracellular vesicles and particles, proteomics, small EVPs

1 | INTRODUCTION

Cells release various extracellular vesicles (EVs), including exosomes, microvesicles, and apoptotic bodies, into their surrounding environment. EVs play crucial roles in intercellular communication by transporting bioactive molecules, such as proteins, lipids, RNA, and even DNA fragments, from one cell to another (Morris & Witwer, 2022). Exosomes are typically 30–150 nm in diameter, while microvesicles and apoptotic bodies are larger, ranging from 0.1 to 1 μm and 1 to 5 μm, respectively (Cheng & Hill, 2022). Recent studies have also identified new subpopulations of small and large exosomes (Exo-S and Exo-L, respectively), as well as

a population of non-membranous nanoparticles called exomes. The collective of extracellular vesicles and particles, referred to as 'EVPs' (Hoshino et al., 2020), encompasses both EVs and extracellular particles (EPs), given their similarities in physical or chemical properties and the limitations of current techniques to differentiate them accurately.

EVPs can be found in various body fluids, but the composition of EVPs varies depending on the tissue source that produced them. Since EVPs can be isolated from circulating fluids, such as blood, they have the potential to be employed as diagnostic biomarkers for biological processes and disease conditions (Busatto et al., 2021; Thakur et al., 2022). For example, the profile and cargo of total circulating EVPs changed with high selectivity during aging and exercise in rats, as the levels of BDNF and IL1B (IL-1β) in old rat EVPs increased with aerobic exercise but decreased with other exercise regimens (Barcellos et al., 2020). A recent study of EVPs in proton secretion by human gastric cancer HGT-1 cells found that constituents of the HGT-1 secretome >100 kDa (including EVPs) modulated proton secretion, while smaller constituents had no effect. The study also found that HGT-1 cell-derived EVPs functioned in proton secretion and subsequent gastric acid release by parietal cells, highlighting a role for EVPs in digestion (Mistlberger-Reiner et al., 2023).

Accordingly, the contents of EVPs collected from a range of body fluids can mirror the physiological and pathological states of tissues and organs, providing valuable insight into the molecular basis of diseases and the effects of therapies (Berumen Sanchez et al., 2021; de Freitas et al., 2021; Huang, Driedonks, Cheng, Rajapaksha, Routenberg, et al., 2022; Lim et al., 2020; Muth et al., 2015; Newman et al., 2022). For instance, EV proteins, DNA, and RNA have been proposed as biomarkers of brain gliomas (Nikoobakht et al., 2021), while various EV proteins, including EGFR, VEGF, CD63, CD24, ADAM10, and ANXA6, have been reported as potential biomarkers for different stages of breast cancer (Li et al., 2021). The ratios of *Y* RNA family members (*Y1*, *Y3*, and *Y4*) in EVs strongly correlated with the numbers and types of immune cells during systemic inflammation, highlighting the value of EVs as diagnostic markers in inflammatory and immune diseases (Driedonks et al., 2020), while non-coding RNAs in liver EVs were used as diagnostic and prognostic biomarkers for hepatocellular carcinoma (Costanzi et al., 2021). Analysis of plasma EV RNAs indicated that *PTEN* mRNA levels were higher in EVs from gastric cancer patients treated with chemotherapy than in EVs from control patients, and that the levels of *FASN* and *CD44* mRNAs decreased after gastrectomy (Rhode et al., 2021). In addition, microRNA profiling of plasma (EpCAM+) EVs from colorectal cancer patients contained reduced levels of eight microRNAs, including miR-16-5p and miR-23a-3p, after surgical removal of the cancer (Ostenfeld et al., 2016); other microRNAs in EVs were also found to be potential biomarkers or effectors in reproductive tract diseases (Zhao et al., 2020).

Despite the potential value of EVPs in circulation, their extreme heterogeneity in size and content makes it difficult to determine their organ of origin. Therefore, we hypothesized that small (s)EVPs (<100 nm) can migrate from various tissues to the bloodstream bearing protein markers that are selective to each organ. To investigate this possibility, we sought to detect highly enriched proteins in sEVPs generated by six organs (brain, liver, lung, heart, kidney, and fat). Our results indicated that each organ produced distinct sEVP proteins, with 68 proteins preferentially found in brain sEVPs, 194 in liver, 39 in lung, 15 in heart, 29 in kidney, and 33 in fat. We then collected serum sEVPs and identified proteins associated with sEVPs in each organ, including brain (DPP6, SYT1, and DNM1L), liver (FABPL, ARG1, and ASGR1/2), lung (SFPTA), heart (CPT1B), kidney (SLC31), and fat (GDN). We further discovered altered levels of these proteins in serum sEVPs from old mice compared to young mice. In sum, we have identified organ-selective sEVP proteins and present evidence that these proteins can be identified in sEVPs in the bloodstream, potentially leading to improved diagnosis of organ-specific conditions.

2 | METHODS

2.1 | Mice

The procedures for importing, housing, conducting experiments, and euthanizing mice were all performed in accordance with the Animal Study Proposal ASP #474-LGG-2023 and its amendments, reviewed and approved by the NIA's Animal Care and Use Committee (ACUC). Young (3 months old, m.o.) and old (24 m.o.) mice, strain C57BL/6JN (NIA aged rodent colony), were given unlimited access to standard chow and kept under a 12-h-light and 12-h-dark cycle.

2.2 | Organ dissociation and sEVP isolation

Mouse organs were dissociated and sEVPs isolated by enzymatic digestion and ultracentrifugation as described (Hurwitz et al., 2019). Briefly, whole-mouse organs (brain, liver, lung, heart, kidney, and fat) were collected after perfusion with sterile PBS. The organs were then incubated in dissociation buffer (10 mg papain, 5.5 mM L-cysteine, 67 μM 2-mercaptoethanol, and 1.1 mM EDTA) at 37°C in Hibernate-E medium for 20 min (Hurwitz et al., 2019) and dissociated with a loose-fit Dounce homogenizer after adding protease and phosphate inhibitors, followed by two rounds of centrifugation at 2500 × g for 10 min at 4°C to remove debris. To begin the isolation of sEVPs, the supernatant was centrifuged at 10,000 × g for 1 h at 4°C to remove apoptotic bodies and microvesicles, and then passed through a 0.22-μm filter (Millipore Sigma, SLGS033SS) to remove debris. We used

ultracentrifugation to isolate sEVPs after the removal of tissue debris and spun the supernatant at 100,000 × g for 2 h at 4°C (Cheng & Hill, 2022; Crescitelli et al., 2021; Huang, Driedonks, Cheng, Rajapaksha, Turchinovich, et al., 2022; Saludas et al., 2022). The sEVPs in the resulting pellet were washed with filtered phosphate-buffered saline (FPBS) and re-ultracentrifuged at 100,000 × g for 1 h at 4°C. It is important to note that further sorting of the isolated sEVPs (Crescitelli et al., 2021) by density gradient or size-exclusion chromatography was not performed to preserve the yield of EVPs for mass spectrometry (MS) analysis. A total of eight mice were used, and EVPs prepared from two sets of four mice each were combined for two different MS analyses. These data are deposited in EV-TRACK knowledgebase (EV-TRACK ID: EV230596) (Consortium EV-TRACK, 2017).

2.3 | sEVP isolation from serum

Mouse blood was collected and allowed to clot for 2 h at 25°C. The blood samples were then centrifuged for 20 min at 2000 × g to obtain the serum. The samples were further centrifuged at 2500 × g for 10 min at 4°C and the supernatants were then subjected to another round of centrifugation at 10,000 × g for 1 h at 4°C to remove apoptotic bodies and microvesicles. The resulting supernatants were passed through a 0.22-μm filter before sEVPs were collected through ultracentrifugation at 100,000 × g for 2 h at 4°C. The sEVPs were then washed using FPBS and subjected to another round of ultracentrifugation at 100,000 × g for 1 h at 4°C. It is important to note that, as above, further sorting of the isolated sEVPs using density gradient or size exclusion chromatography was not performed to maintain the yield for mass spectrometry analysis.

2.4 | Nanoflow cytometry (NFCM)

The size distribution of the isolated EVPs was determined using NFCM technology, the Flow NanoAnalyzer from NanoFCM, Inc. The procedure was performed following the methodology previously described (Huang, Driedonks, Cheng, Rajapaksha, Routenberg, et al., 2022). Briefly, the instrument was calibrated with 250-nm Silica Beads and a Silica Nanosphere Cocktail to determine particle concentration and size, respectively. Particle count and size were determined using the calibration curve, flow rate, and side scatter intensity, and events were recorded for one minute, following the manufacturer's guidelines for NanoFCM operation.

2.5 | ExoView analysis

We assessed surface marker proteins using ExoView R200 (NanoView Biosciences) following the manufacturer's recommendations. Briefly, we incubated equal concentrations of EVP samples (50 μL) on ExoView Tetraspanin chips in a 24-well plate for 16 h. After the chip was washed three times with 1× Solution A, we added 250 μL of detection antibodies (anti-CD9 and anti-CD81) in blocking buffer for 1 h. The chip was washed twice with solution A, followed by three washes with solution B, and finally with deionized water. After drying on absorbent paper, the chips were scanned with ExoView R200 and analyzed using ExoScan software (NanoView Biosciences).

2.6 | Transmission electron microscopy

For TEM analysis, 20 μL of sEVP samples (around 10^{10} particles/mL) in suspension were adsorbed to carbon-coated parlodion copper grids for 2 min, then the grids were floated on 2 consecutive drops of filtered aqueous 0.75% uranyl acetate (0.03% tylose) for 1 min each and blot-dried with filter paper. After the adsorption step, the sEVPs were fixed on poly-L-lysine coverslips using 1% glutaraldehyde 80 mM phosphate buffer containing 5 mM $MgCl_2$. Coverslips were rinsed in buffer with sucrose then postfixed in potassium ferrocyanide-reduced osmium tetroxide for 1 h on ice. Samples were stained en bloc in 2% uranyl acetate in maleate buffer for 1 h. After a series of progressive ethanol dehydration steps (30%–100%), samples were infiltrated with Eponate 12 resin, embedded, and cured at 60°C for 48 h. After soaking in liquid nitrogen for 10 min, coverslips mounted to inverted beam capsules were carefully removed. On a Riechart Ultracut E microtome, blocks were trimmed and sectioned with a diatome diamond knife. Methanolic uranyl acetate was used to stain sections (50-60 nm), followed by incubation with lead citrate. After rinsing, the grids (coverslips) were hard-fixed in 2% glutaraldehyde in 100 mM sodium cacodylate buffer, stained with 2% uranyl acetate for 20 min, and rinsed in between with distilled water. Finally, the grids were viewed on a Hitachi H 7600 TEM operating at 80 kV and digital images were captured using an XR50 5-megapixel CCD camera from Advanced Microscopy Techniques Corp.

2.7 | Mass spectrometry-based proteomics of EVPs

For proteomic analysis of sEVPs, four mice were utilized to isolate sEVPs from various organs (brain, liver, lung, heart, kidney, and fat) and blood serum; this isolation process was repeated twice and whole-sEVP proteins were then extracted for MS analysis without density gradient or size exclusion, as described (Crescitelli et al., 2021). Briefly, proteins were extracted from the pellets of EVPs, and the concentration was measured using a Pierce MicroBCA kit. Each sample was processed by treating 20 μg of protein with DTT for reduction, subsequently with iodoacetamide for alkylation, and finally digested with trypsin in a 25 mM NH_4HCO_3 solution. The resulting tryptic peptide mixtures were cleaned with a C18 column and reconstituted in 25 μl of 0.1% formic acid; 12 μl of this mixture was then analyzed using 110 min LC/MS/MS.

LC/MS/MS analysis was conducted using a Thermo Scientific Orbitrap Exploris 240 Mass Spectrometer and a Thermo Dionex UltiMate 3000 RSLCnano System. The Orbitrap Exploris 240 instrument operated in a data-dependent mode, switching between full scan MS and MS/MS acquisition automatically. Peptide mixtures from each sample were loaded onto a peptide trap cartridge at a flow rate of 5 μL/min. The trapped peptides were then eluted onto a reversed-phase EasySpray C18 column (Thermo Fisher Scientific) using a linear gradient of acetonitrile (3-36%) in 0.1% formic acid over a duration of 110 min at a flow rate of 0.3 μL/min. Eluted peptides from the EasySpray column were ionized and sprayed into the mass spectrometer using a Nano-EasySpray Ion Source (Thermo Fisher Scientific) with the following settings: spray voltage of 1.6 kV and capillary temperature of 275°C. The 15 most intense multiply charged ions ($z \geq 2$) were sequentially isolated and fragmented in the octopole collision cell using higher-energy collisional dissociation (HCD) with normalized HCD collision energy of 30. The AGC target was set to 10^5, and the maximum injection time was 200 ms at a resolution of 17,500. The isolation window was set to 2, and a dynamic exclusion of 20 seconds was applied. Charge state screening was enabled to reject unassigned ions as well as ions with 1+ and 7+ or higher charge states.

Raw data files from each sample were searched against the mouse protein sequence database from the UniprotKB/Swiss-Prot database using the Proteome Discoverer (v1.4) and the SEQUEST algorithm (Thermo Fisher Scientific). A minimum peptide length of 5 amino acids and a maximum false peptide discovery (FDR) rate of 0.01 were specified. All assembled proteins with peptide spectrum match (PSM) counts were quantified and normalized using the normalized spectral abundance factors (NSAFs) to determine their relative abundance.

2.8 | Western blot analysis

Proteins were extracted from sEVPs using a denaturing buffer that contained 2% SDS (Sigma-Aldrich) in 50 mM HEPES. The samples were subjected to sonication, followed by centrifugation at 4°C for 10 min at 12,000 × g to obtain whole-sEVP protein lysates. The protein concentration was determined using a Pierce BCA Protein Assay Kit (Thermo Fisher Scientific). Equal amounts of the extracted sEVP proteins were boiled in sample buffer and then separated by size through polyacrylamide gels (10 μg/well) and transferred to nitrocellulose membranes (Bio-Rad). The membranes were blocked with 5% nonfat dry milk and used for western blot analysis. Specific primary antibodies were employed to recognize SYT1 (ABclonal, A0992), DPP6 (Abcam, ab198506), DNM1L (DRP1, Cell Signaling, 14647), ARG1 (Cell Signaling, 93668), ASGR1/2 (Santa Cruz Biotechnology, sc-166633), FABPL (Cell Signaling, 13368T), CPT1B (ThermoFisher, 22170-1-AP), GDN (ABclonal, A14540), SFPTA (ABclonal, A3133), and SLC31 (ABclonal, A5500). The membranes were then incubated with respective secondary antibodies (1:10,000, KwikQuant from Kindle Biosciences) and the signals developed using enhanced chemiluminescence (ECL). The images were captured using ChemiDoc MP (Bio-Rad). Western blot images were analyzed using the ImageJ software. The intensity of each protein band was quantified using the 'Measure' function in ImageJ.

2.9 | Statistical analysis and graphs

The experiments were conducted in biological triplicates, unless otherwise specified. The data were analyzed using unpaired Student's *t*-test. Statistical significance was denoted as follows: $^*p < 0.05$; $^{**}p < 0.01$; $^{***}p < 0.001$. Graphs were generated using GraphPad Prism 9.

3 | RESULTS

3.1 | Quality control of organ sEVPs

For sEVP isolation, we harvested six organs (brain, liver, lung, heart, kidney, and fat) from each mouse (Figure 1a). The isolated sEVPs (Methods) were subjected to quality control by assessing their size distribution using a NanoFCM instrument (Methods).

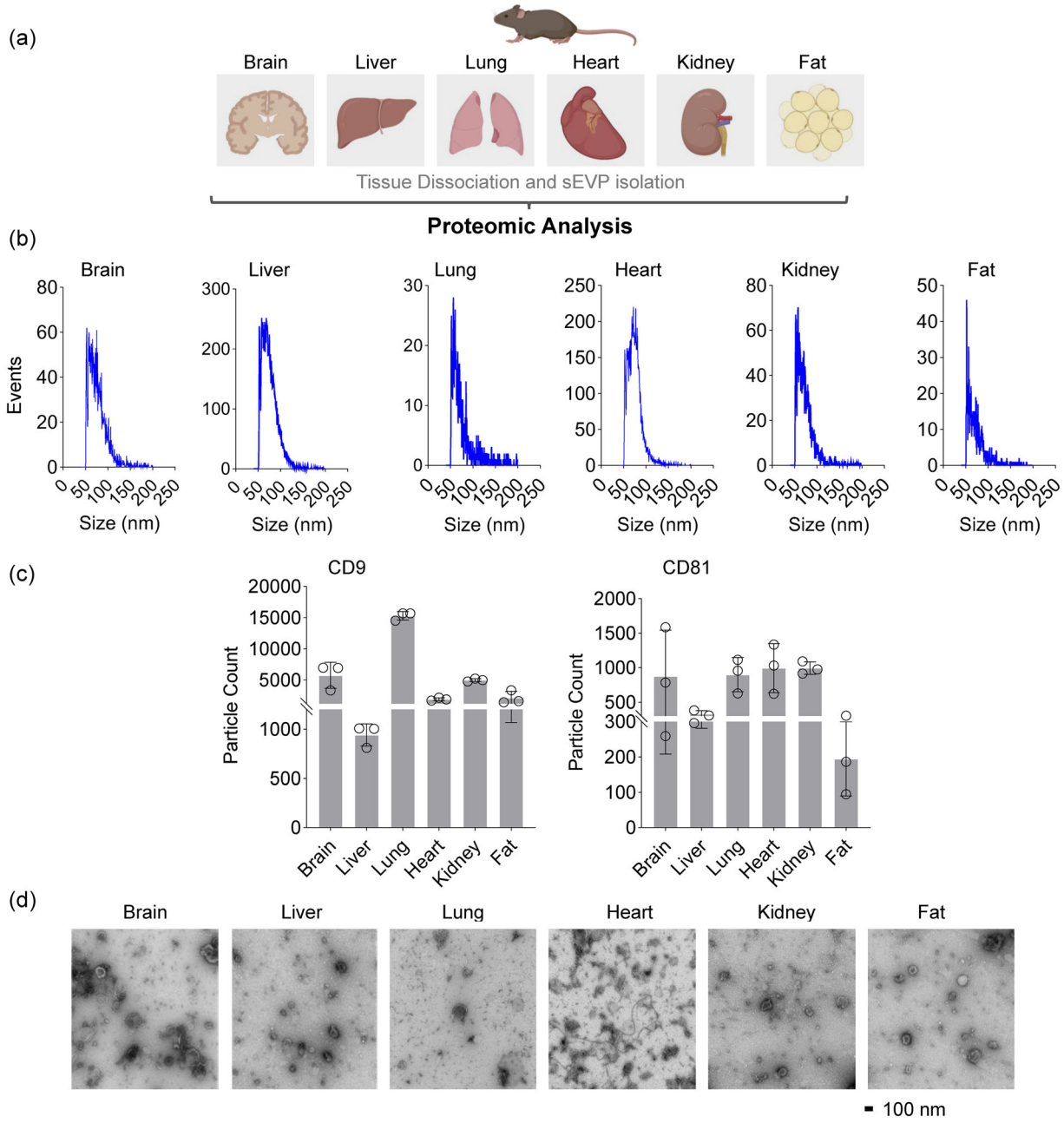

FIGURE 1 **Isolation of sEVPs from organs**. (a) Workflow depicting the organs selected for sEVP isolation and subsequent proteomic analysis (Methods). (b) The size distribution of the collected sEVPs from the specified organs in (a) as assessed using a NanoFCM instrument. (c) Proteins CD9 and CD81 were detected in EVPs from the indicated organs using NanoView (Methods). (d) Representative Transmission Electron Microscopy (TEM) images of sEVPs isolated from the organs outlined in (a).

As shown (Figure 1b), all sEVPs displayed a similar range of diameters (50–100 nm). It is noteworthy that we focused on this size range of sEVPs as these can cross the blood-brain barrier (Banks et al., 2020; Ramos-Zaldivar et al., 2022), and are therefore likely capable of traveling from various tissues to the bloodstream. We confirmed the presence of the tetraspanins CD9 and CD81 in sEVPs isolated from these organs (Figure 1c). Imaging using TEM (Figure 1d) further confirmed the presence of sEVPs isolated from these organs, and we set out to characterize the proteins in sEVPs by MS analysis.

3.2 | sEVP protein contents reflect the parent organ of origin

To investigate the protein contents of sEVPs isolated from each organ, we combined four isolations together for improved mass spectrometry coverage. Proteomic analysis identified and quantified proteins in sEVPs isolated from each organ (Figure 2a,

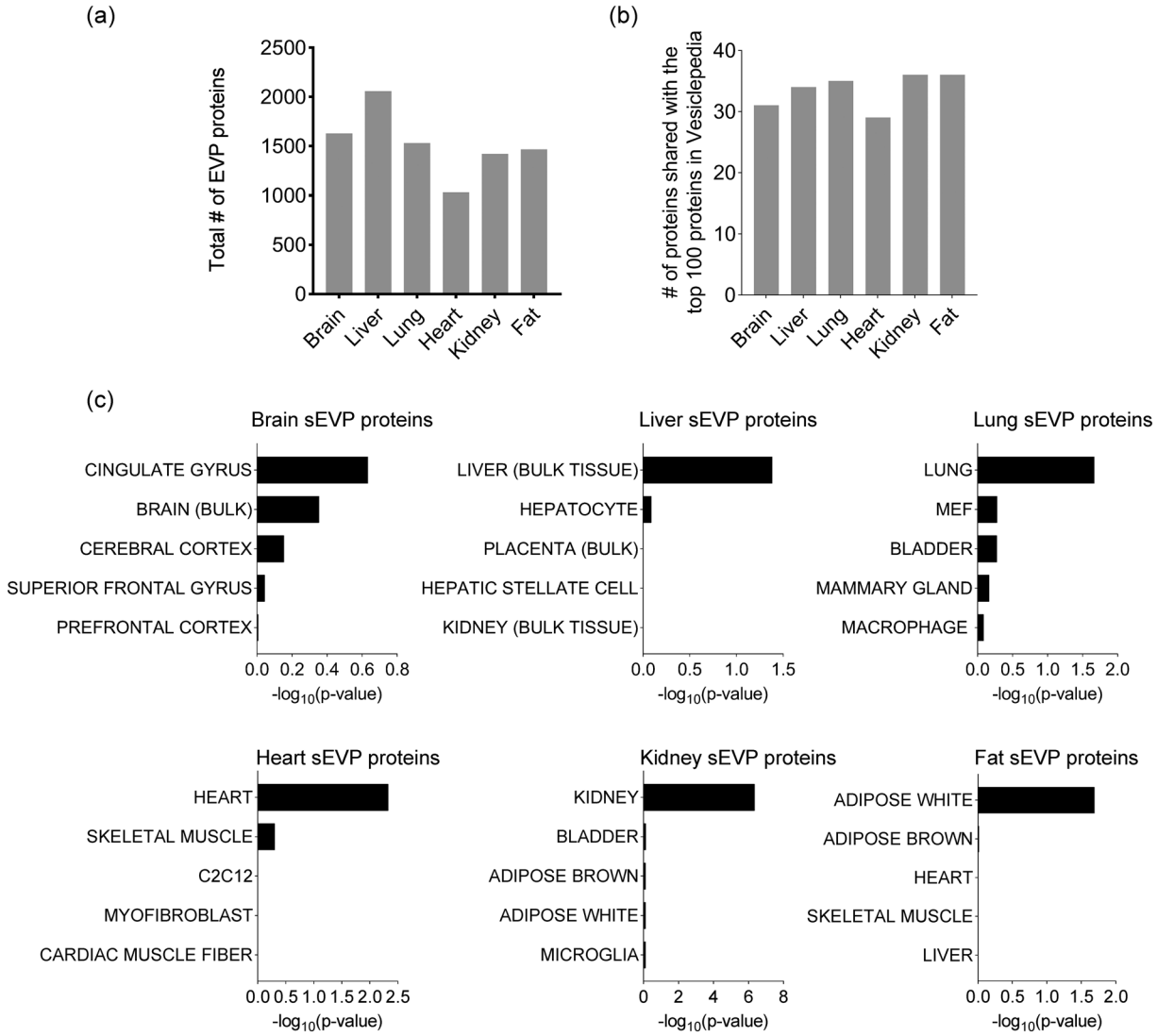

FIGURE 2 **Mass spectrometry profiling of proteomes of organ-derived sEVPs**. (a) Bar graph indicating the number of proteins identified by proteomic analysis. (b) Bar graph representation of the number of sEVP proteins overlapping with the top 100 EV proteins in the Vesiclepedia database. (c) Protein datasets were tested for enrichment for different cell types against mouse gene atlas on the Enrichr platform. The main enriched cell types for each sEVP protein dataset from the indicated organs are shown.

Supplementary Table 1, and **MSV000091839** at https://massive.ucsd.edu). A comparison of our datasets with the top 100 EV proteins in the Vesiclepedia database (microvesicles.org) revealed the presence of EV proteins among the total number of proteins obtained from each sample (Figure 2b and Supplementary Table 2). EVs are believed to serve as a 'fingerprint' of the originating cells (Thakur et al., 2022). To determine if the protein content of sEVPs reflects the organ of origin, we used the Enrichr mouse atlas cell type enrichment algorithm to analyze the protein content of sEVPs isolated from individual organs. The results confirmed that sEVPs from each organ provide a distinct fingerprint for their origin (Figure 2c). Together, these findings confirm the presence of known and novel proteins in the collection of sEVPs and support the notion that the presence of distinctive proteins can be used to assign each sEVP population to its respective organ of origin.

3.3 | Proteome analysis reveals shared and distinct sEVP proteins across the organs

Next, we analyzed the different protein datasets to identify shared as well as selectively enriched sEVP proteins among the six organs. We used UpSet plots to visualize the overlapping sEVP proteins among the six organs. For example, lung and fat shared 189 sEVP proteins, while lung and heart shared only 2 sEVP proteins. On the other hand, liver, fat, and lung shared 104 sEVP proteins, while liver, lung, and heart combined shared shared 3 sEVP proteins sEVP proteins (Figure 3a). Furthermore, the UpSet

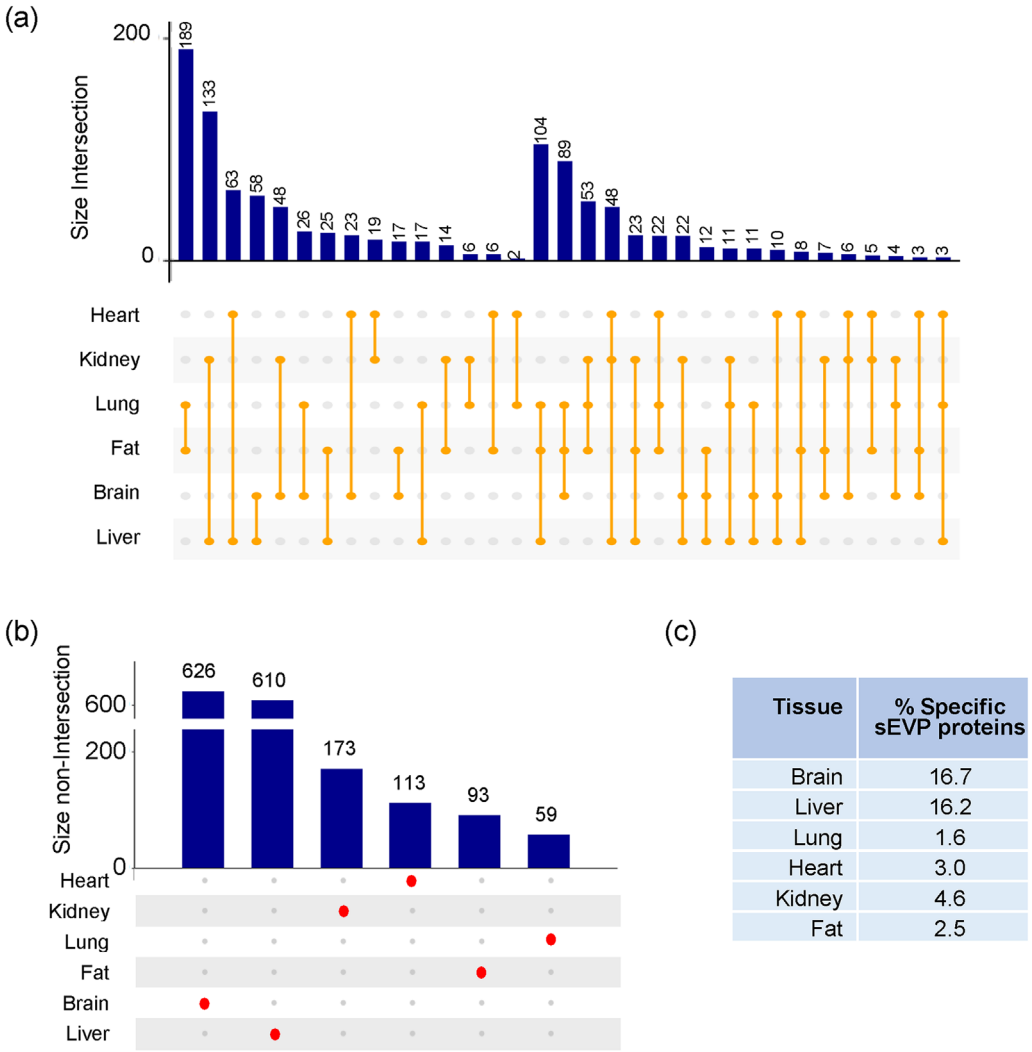

Tissue	% Specific sEVP proteins
Brain	16.7
Liver	16.2
Lung	1.6
Heart	3.0
Kidney	4.6
Fat	2.5

FIGURE 3 **Distinct and shared sEVP proteins**. (a) UpSet plot of the proteomic datasets to visualize all the combinations of intersections indicating common proteins detected in sEVPs from two or more organs. (b) UpSet plot of the proteomic datasets to visualize selective sEVP proteins within individual organs. (c) Percentages of sEVP proteins preferential to each individual organ, not shared with other organs, out of a total of 3753 proteins present in all tissue samples.

plot also showed sEVP proteins selectively enriched in individual tissue samples, out of 3753 total proteins: 626 in brain (16.7% of the total), 610 in liver (16.2%), 173 in kidney (4.6%), 113 in heart (3%), 93 in fat (2.5%), and 59 in lung (1.6%) (Figure 3b,c). These results uncovered different numbers of shared sEVP proteins among the organs, and also showed the number of enriched sEVP proteins present in each organ, with the brain and liver having the highest number of selectively enriched sEVP proteins. This variation could be attributed to the size of the organs or the difficulty in efficiently dissociating organs like the heart.

3.4 | Organ-derived sEVP proteins

To ascertain the enrichment of organ-derived sEVP proteins, we evaluated their degree of exclusivity. Proteins that were exclusively found in one organ with no peptides detected in other organs were considered to have 100% organ exclusivity; highly distinct proteins displaying 90–99% exclusivity for a specific organ were also included in the analysis.

As shown, several sEVP proteins found in the brain appeared to be highly exclusive to the brain, with 100% exclusivity for proteins like SYT1 (synaptotagmin-1) and DPP6 (dipeptidyl aminopeptidase-like protein 6). Additionally, DNM1L (dynamin-1-like protein), a protein with 97% exclusivity in brain sEVPs, showed only one detected peptide in the sEVPs from the kidney. (Figure 4a and Supplementary Table 3). In the liver, several sEVP proteins were identified with 100% exclusivity, such as arginase-1 (ARG1) and asialoglycoprotein receptors 1 and 2 (ASGR1/2). Other liver sEVP proteins displayed 92–98% exclusivity, such as fatty

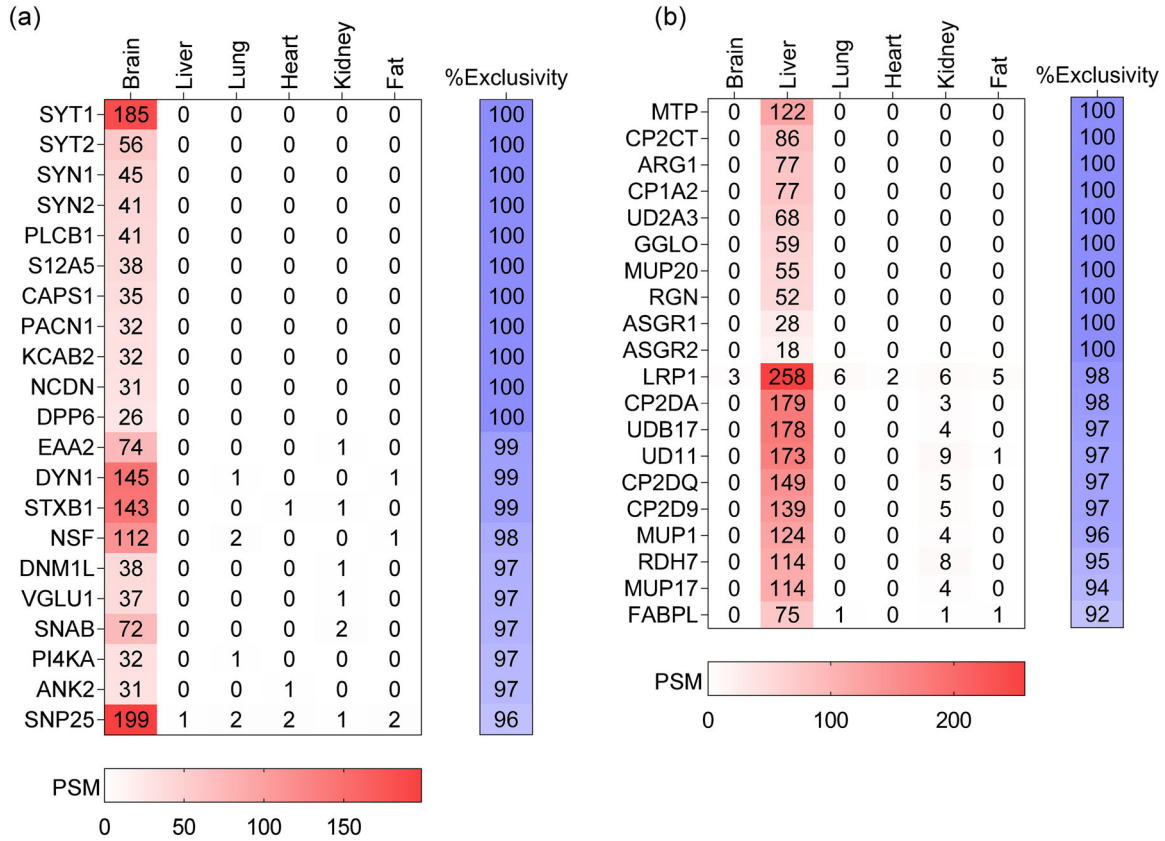

FIGURE 4 sEVP proteins preferential to brain and liver. Heatmaps of proteins and PSM (peptide-spectrum match) counts exclusive (100%) or highly selective (90-99%) to sEVPs from brain (a) and liver (b).

acid-binding protein 1 (FABPL), for which only one peptide was detected in sEVPs from lung, kidney, and fat (Figure 4b and Supplementary Table 4).

In lung sEVPs, proteins like surfactant pulmonary-associated protein A (SFTPA) showed 100% exclusivity, while 94–96% exclusivity was seen for proteins like advanced glycosylation end-product-specific receptor (RAGE) (Figure 5a and Supplementary Table 5). Heart sEVPs displayed 100% exclusivity for proteins such as myosin heavy chain 6 (MYH6), and 92–99% exclusivity for proteins like carnitine palmitoyltransferase 1b (CPT1B) (Figure 5b and Supplementary Table 6). Furthermore, 100% exclusivity was found for some kidney sEVP proteins, including solute carrier family 3 member 1 (SLC31, also known as neutral and basic amino acid transport protein rBAT or NBAT), and highly selective proteins (92 to 99%) like carboxypeptidase M (CBPM) (Figure 5c and Supplementary Table 7). Finally, in fat sEVPs, proteins like serpin family E member 2 (SERPINE2; also known as GDN) were among those exclusively expressed, while another fat sEVP protein, laminin alpha 4 (LAMA4), showed high selectivity (92%–94%) (Figure 5d and Supplementary Table 8). Together, these findings highlight the usefulness of proteomic analysis in identifying shared and organ-preferential sEVP proteins.

3.5 | Detection and validation of organ-derived sEVP proteins in serum

As shown above, proteomic analysis identified organ-selective sEVP proteins with 90 to 100% exclusivity (Figures 4 and 5). However, when these sEVPs reach the bloodstream, it is difficult to identify their organs of origin. To begin to address this hurdle, we combined five isolates of mouse serum sEVPs in duplicate, to enhance the coverage in proteomic analysis (Figure 6a). The quality and size distribution of isolated serum sEVPs were then evaluated using a NanoFCM (Methods). The results indicated that serum-derived sEVPs had a diameter of 50–100 nm (Figure 6b). We also confirmed the presence of the tetraspanin surface proteins CD9 and CD81 in EVPs isolated from serum using NanoView as shown in Figure 6c. Furthermore, TEM imaging confirmed the isolation of sEVPs (Figure 6d), allowing for downstream characterization of mouse serum sEVP proteins through MS analysis (Figure 6e and Supplementary Table 9). A comparison of serum sEVP proteins with the top 100 EV proteins in the Vesiclepedia database (microvesicles.org) indicated the presence of EV proteins among the total number of proteins (Figure 6e and Supplementary Table 2). Next, we sought to identify highly selective sEVP proteins (90-100%) in serum sEVP proteins. This

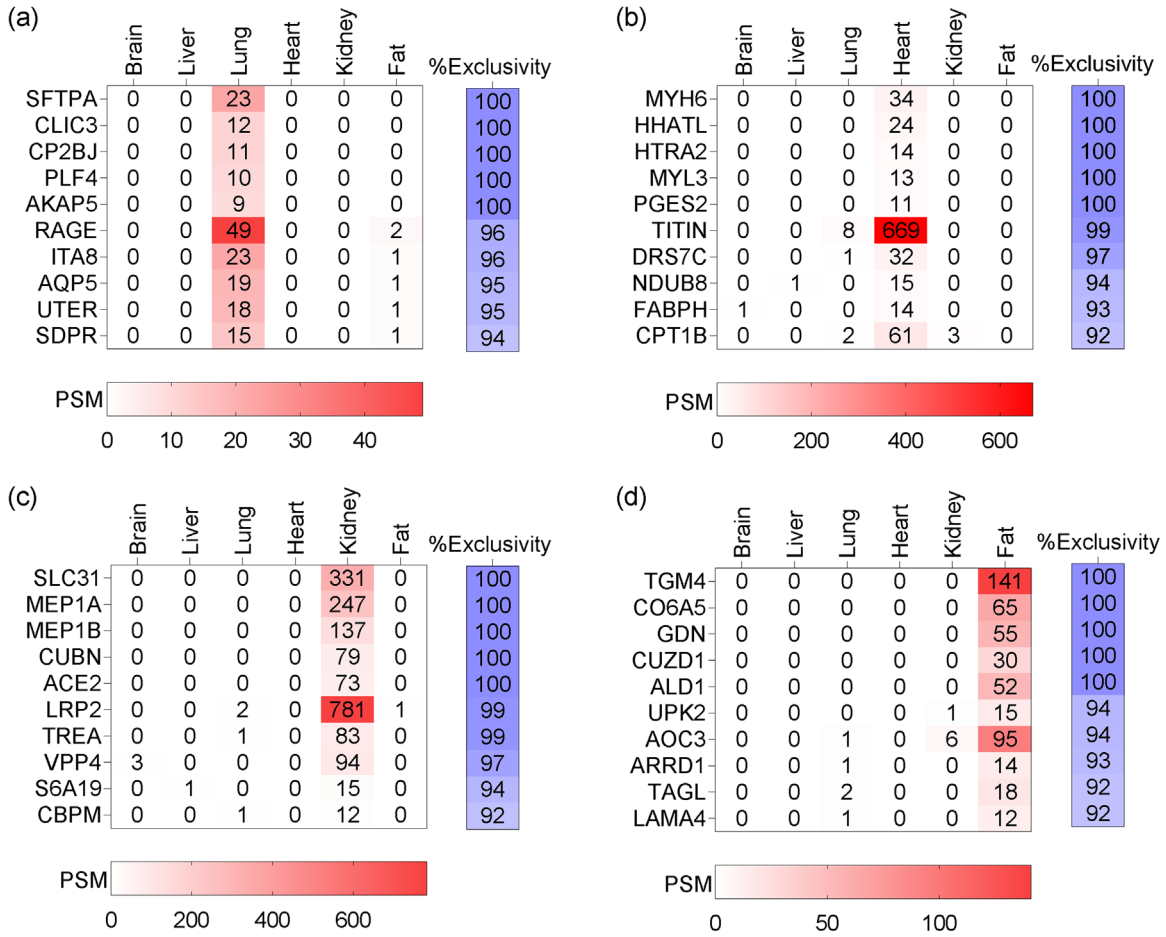

FIGURE 5 sEVP proteins preferential to lung, heart, kidney, and fat. Heatmaps of proteins exclusive (100%) or highly specific (90-99%) to sEVPs from lung (a), heart (b), kidney (c), and fat (d).

analysis indicated that serum sEVP proteins included 68 sEVP proteins preferential to brain, 194 to liver, 39 to lung, 15 to heart, 29 to kidney, and 33 to fat (Figure 6f and Supplementary Table 10).

Next, we validated a subset of these sEVP proteins using commercially available antibodies. Western blot analysis confirmed the presence of SYT1, DNM1L, and DPP6 in protein lysates obtained from brain and serum sEVPs. Similarly, ARG1, FABPL, and ASGR1/2 were expressed in protein lysates obtained from liver and serum sEVPs. We also validated the presence of SFTPA in lung and serum sEVP lysates, and the presence of CPT1B in heart and serum sEVP lysates. SLC31 was preferentially expressed in kidney and serum sEVP lysates, and GDN was expressed in fat and serum sEVP lysates (Figure 6g, Supplementary figure S1). Together, these findings indicate that these organ-selective sEVP proteins can be found within the population of sEVPs isolated from serum.

3.6 | Altered organ-selective sEVP proteins in serum with age

Next, we extended these findings to evaluate the changes of organ-selective sEVP proteins in serum as a function of age. We isolated sEVPs from serum of young (3 months old, m.o.) and old (24 m.o.) mice and performed western blot analysis. As shown (Figure 7, Supplementary figure S2), aging influenced the levels of sEVP proteins in various organs. In serum sEVPs obtained from old mice, the preferential brain sEVP proteins SYT1 and DPP6 were less abundant, while DNM1L was more abundant than in serum sEVPs from young mice. On the other hand, the liver-derived sEVP proteins ASGR1/2 and ARG1 were more abundant, while FABPL was less abundant in serum sEVPs from old mice compared to young. Furthermore, the proteins distinctive for sEVPs from lung (SFTPA), heart (CBT1B), kidney (SLC31), and fat (GDN), were all increased in serum sEVPs obtained from old mice. These data highlight a useful application of the identification of organ-derived sEVP protein markers, which allows a rapid and defined survey of serum sEVPs and their organ of biogenesis.

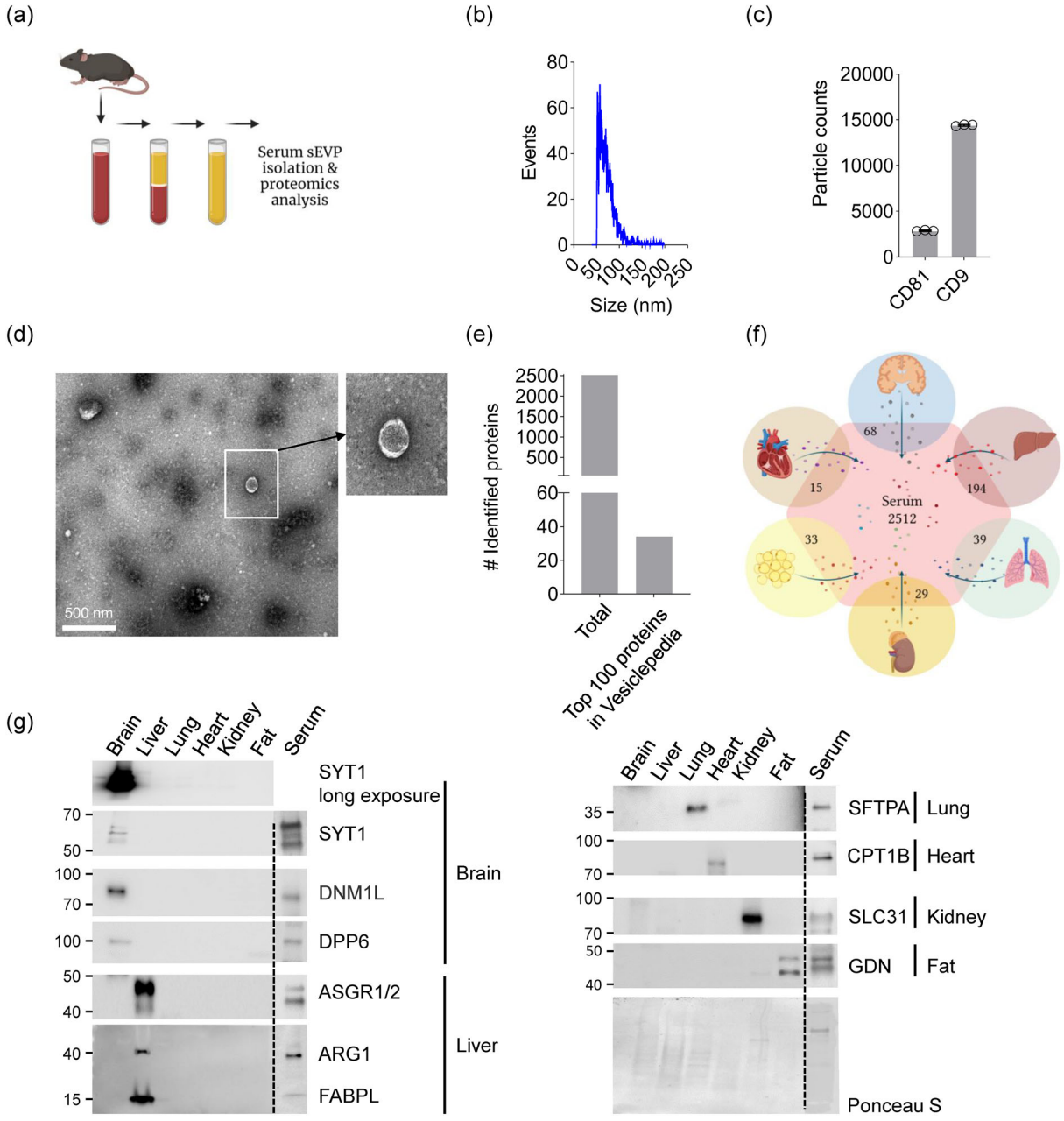

FIGURE 6 **Organ-derived sEVP proteins in serum**. (a) Workflow employed to isolate sEVPs from blood serum used to perform proteomic analysis (Methods). (b) Size distribution of sEVPs collected from mouse serum described in (a), as measured by NanoFCM (Methods). (c) CD9 and CD81 proteins were detected in EVPs from serum using NanoView (Methods). (d) Representative TEM image showing sEVPs isolated from serum. (e) Bar graph indicating the number of serum sEVP proteins detected by MS analysis overlapping with the top 100 EV proteins in Vesiclepedia database. (f) Venn diagram indicating the intersections between organ-specific sEVP proteins (Figures 4 and 5) and serum sEVP proteomics. (g) Western blot analysis of the levels of SYT1, DNM1L, DPP6, ASGR1/2, ARG1, FABPL, SFTPA, CPT1B, SLC31, and GDN using sEVP lysates from the indicated organs. The overall loading and transfer of samples (10 μg/well) were monitored by staining the membranes with Ponceau S. Numbers on the left of the blots indicate the positions of molecular weight markers.

4 | DISCUSSION

More extensively investigated than EVPs, EVs have emerged as informative biological structures released by tissues and organs across the body to the extracellular space, carrying macromolecules such as DNA, RNA, proteins, and lipids. Secreted EVs can enter the bloodstream and cross the blood-brain barrier, and their contents may reveal information about the origin, function, and pathological conditions of the cells from which they originated (Saint-Pol et al., 2020; van Niel et al., 2022). Since EVs are abundant in body fluids such as blood, urine, saliva, and breast milk, they can be readily collected and utilized for the diagnosis of a range of pathologies, including neurodegenerative diseases and cancer (Shetty & Upadhya, 2021). While blood EVs can help

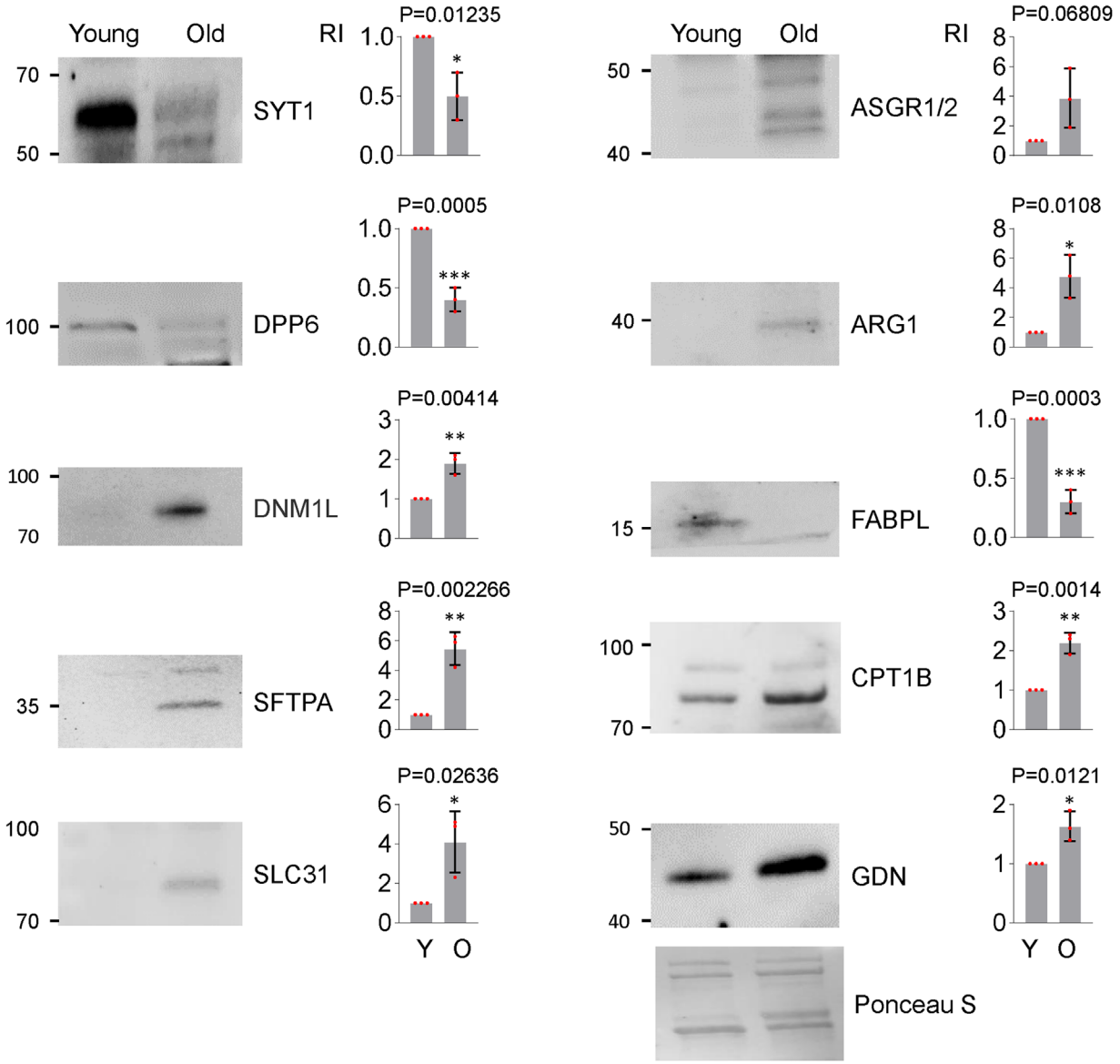

FIGURE 7 **Changes in organ-derived sEVP proteins in serum as a function of age**. Western blot analysis (left) and quantification of intensity of the bands (right) were used to assess the levels of SYT1, DNM1L, DPP6, ASGR1/2, ARG1, FABPL, SFTPA, CPT1B, SLC31, and GDN in sEVPs from serum of young (Y; 3 months old, m.o.) and old (O; 24 m.o.) mice. The global loading and transfer of samples (10 μg/well) were monitored by staining the membranes with Ponceau S. Quantification of the bands obtained by western blot analysis (using ImageJ) in three independent experiments was used to calculate the relative intensity (RI). Numbers on the left of the blots indicate the positions of molecular weight markers. Data were analyzed using unpaired Student's *t*-test. Statistical significance was indicated as follows: $^{*}p < 0.05$; $^{**}p < 0.01$; and $^{***}p < 0.001$.

monitor physiological and pathological conditions, the tissues and organs of origin of circulating EVs are largely unknown due to their high level of heterogeneity in the blood (Bordanaba-Florit et al., 2021; Dechantsreiter et al., 2022; Willms et al., 2018). Thus, identification of the specific EV protein markers in different tissues and organs is urgently needed (Gomes & Witwer, 2022).

Here, we surveyed sEVP (50-100 nm) proteins from six mouse organs—brain, liver, lung, heart, kidney, and fat. Given that organ-selective sEVPs retain their protein identity as they travel into the bloodstream, we performed proteomic analysis using sEVPs isolated from these organs and serum. We identified sEVP proteins that were both (i) exclusively or highly selective to a single organ within these limited comparisons, and (ii) detectable in serum sEVPs, in order to create a protein catalog that can serve for the noninvasive, rapid detection of diagnostic biomarkers of various organs through small particles present in the blood.

Using a mouse aging model, we monitored age-related changes in the content of organ-derived sEVP proteins in serum sEVPs. Among these proteins, we identified brain sEVP proteins DPP6 and SYT1 as being reduced with age in serum sEVPs, while brain sEVP protein DNM1L was increased in serum sEVPs of old mice. Interestingly, DPP6 loss was associated with neuronal hyperexcitability and neurodegenerative dementia (Cacace et al., 2019), while increased DPP6 levels contributed to a deficit in

neurotransmission in an iPSC model of schizophrenia (Naujock et al., 2020). SYT1 levels decreased in AD brains due to synaptic loss (Zoltowska et al., 2017), while they were elevated in the cerebrospinal fluid of patients with AD, and thus SYT1 might serve as a disease biomarker (Ohrfelt et al., 2016); similarly, increased levels of DNM1L were found in metabolic diseases and neuronal damage (Oliver & Reddy, 2019). The liver fatty acid-binding protein FABPL was downregulated in serum sEVPs obtained from old mice, and its reduction was previously linked to reduced hepatic fatty acid uptake and increased obesity (Atshaves et al., 2010). On the other hand, the liver sEVP protein ARG1, which was found elevated in serum sEVPs from old mice, has been described as a potential marker of steatosis (Alisi et al., 2015) and HCC progression (Fujiwara et al., 2012).

This study aimed to analyze sEVP proteins from organs and serum samples through a process of filtration and ultracentrifugation (without further sorting into subpopulations) to gather enough material for high-throughput proteomic analysis. In future experiments, using far larger starting materials, we will endeavor to further purify EVPs into subpopulations (e.g., large and small EVs) using size exclusion chromatography and density gradients. A major limitation of this study was the reduced number of replicates. Therefore, future experiments will focus on substantially expanding the number of mice involved in the study to allow for more replicates for mass spectrometry analysis. Future experiments will also aim to identify serum EVP proteins originating from additional organs, such as muscle, skin, pancreas, spleen, and intestine, as well as from individual tissue types from those organs, possibly down to single-cell analysis of EVPs. Beyond characterizing sEVPs from organs in physiologic conditions, further studies will focus on identifying EVPs from disease states in different organs, and will expand on the roles of EVP proteins in parent organs during aging and age-related diseases. Finally, to elucidate the complete catalog of potential organ-selective EVP biomarkers, it will also be essential to identify the nucleic acids and lipids of EVPs originating from specific organs. These signatures may ultimately be useful for identifying human blood EVPs and expand the repertoire of physiologic and disease processes for which EVs offer valuable prognostic and diagnostic information.

ACKNOWLEDGEMENTS

This work was supported by the National Institute on Aging Intramural Research Program of the National Institutes of Health. We thank KW Witwer and O Gololobova (Johns Hopkins University School of Medicine) for assistance with NanoFCM analysis and valuable discussions. We thank Nirad Banskota and Stefano Donega (NIA) for help with data processing. National Institute on Aging Intramural Research Program, National Institutes of Health.

CONFLICT OF INTEREST STATEMENT

The authors declare no conflict of interest.

ORCID

Kotb Abdelmohsen https://orcid.org/0000-0001-6240-5810
Myriam Gorospe https://orcid.org/0000-0001-5439-3434

REFERENCES

Alisi, A., Comparcola, D., De Stefanis, C., & Nobili, V. (2015). Arginase 1: A potential marker of a common pattern of liver steatosis in HCV and NAFLD children. *Journal of Hepatology*, *62*(5), 1207–1208. https://doi.org/10.1016/j.jhep.2014.12.036

Atshaves, B. P., McIntosh, A. L., Storey, S. M., Landrock, K. K., Kier, A. B., & Schroeder, F. (2010). High dietary fat exacerbates weight gain and obesity in female liver fatty acid binding protein gene-ablated mice. *Lipids*, *45*(2), 97–110. https://doi.org/10.1007/s11745-009-3379-2

Banks, W. A., Sharma, P., Bullock, K. M., Hansen, K. M., Ludwig, N., & Whiteside, T. L. (2020). Transport of extracellular vesicles across the blood-brain barrier: Brain pharmacokinetics and effects of inflammation. *International Journal of Molecular Sciences*, *21*(12), 4407. https://doi.org/10.3390/ijms21124407

Barcellos, N., Cechinel, L. R., de Meireles, L. C. F., Lovatel, G. A., Bruch, G. E., Carregal, V. M., Massensini, A. R., Dalla Costa, T., Pereira, L. O., & Siqueira, I. R. (2020). Effects of exercise modalities on BDNF and IL-1beta content in circulating total extracellular vesicles and particles obtained from aged rats. *Experimental Gerontology*, *142*, 111124. https://doi.org/10.1016/j.exger.2020.111124

Berumen Sanchez, G., Bunn, K. E., Pua, H. H., & Rafat, M. (2021). Extracellular vesicles: Mediators of intercellular communication in tissue injury and disease. *Cell Communication and Signaling*, *19*(1), 104. https://doi.org/10.1186/s12964-021-00787-y

Bordanaba-Florit, G., Royo, F., Kruglik, S. G., & Falcon-Perez, J. M. (2021). Using single-vesicle technologies to unravel the heterogeneity of extracellular vesicles. *Nature Protocols*, *16*(7), 3163–3185. https://doi.org/10.1038/s41596-021-00551-z

Busatto, S., Morad, G., Guo, P., & Moses, M. A. (2021). The role of extracellular vesicles in the physiological and pathological regulation of the blood-brain barrier. *FASEB BioAdvances*, *3*(9), 665–675. https://doi.org/10.1096/fba.2021-00045

Cacace, R., Heeman, B., Van Mossevelde, S., De Roeck, A., Hoogmartens, J., De Rijk, P., Gossye, H., De Vos, K., De Coster, W., Strazisar, M., De Baets, G., Schymkowitz, J., Rousseau, F., Geerts, N., De Pooter, T., Peeters, K., Sieben, A., Martin, J. J., Engelborghs, S., … Consortium, B. (2019). Loss of DPP6 in neurodegenerative dementia: A genetic player in the dysfunction of neuronal excitability. *Acta Neuropathologica*, *137*(6), 901–918. https://doi.org/10.1007/s00401-019-01976-3

Cheng, L., & Hill, A. F. (2022). Therapeutically harnessing extracellular vesicles. *Nature Reviews Drug Discovery*, *21*(5), 379–399. https://doi.org/10.1038/s41573-022-00410-w

Consortium EV-TRACK, Van Deun, J., Mestdagh, P., Agostinis, P., Akay, O., Anand, S., Anckaert, J., Martinez, Z. A., Baetens, T., Beghein, E., Bertier, L., Berx, G., Boere, J., Boukouris, S., Bremer, M., Buschmann, D., Byrd, J. B., Casert, C., Cheng, L., … Hendrix, A.. (2017). EV-TRACK: Transparent reporting and centralizing knowledge in extracellular vesicle research. *Nature Methods*, *14*(3), 228–232. https://doi.org/10.1038/nmeth.4185

Costanzi, E., Simioni, C., Varano, G., Brenna, C., Conti, I., & Neri, L. M. (2021). The role of extracellular vesicles as shuttles of RNA and their clinical significance as biomarkers in hepatocellular carcinoma. *Genes (Basel)*, *12*(6), 902. https://doi.org/10.3390/genes12060902

Crescitelli, R., Lasser, C., & Lotvall, J. (2021). Isolation and characterization of extracellular vesicle subpopulations from tissues. *Nature Protocols*, *16*(3), 1548–1580. https://doi.org/10.1038/s41596-020-00466-1

de Freitas, R. C. C., Hirata, R. D. C., Hirata, M. H., & Aikawa, E. (2021). Circulating extracellular vesicles as biomarkers and drug delivery vehicles in cardiovascular diseases. *Biomolecules*, *11*(3), 388. https://doi.org/10.3390/biom11030388

Dechantsreiter, S., Ambrose, A. R., Worboys, J. D., Lim, J. M. E., Liu, S., Shah, R., Montero, M. A., Quinn, A. M., Hussell, T., Tannahill, G. M., & Davis, D. M. (2022). Heterogeneity in extracellular vesicle secretion by single human macrophages revealed by super-resolution microscopy. *Journal of Extracellular Vesicles*, *11*(4), e12215. https://doi.org/10.1002/jev2.12215

Driedonks, T. A. P., Mol, S., de Bruin, S., Peters, A. L., Zhang, X., Lindenbergh, M. F. S., Beuger, B. M., Stalborch, A. D., Spaan, T., Jong, E. C., Vries, E., Margadant, C., Bruggen, R., Vlaar, A. P. J., Groot Kormelink, T., & Nolte-'t Hoen, E. N. M. (2020). Y-RNA subtype ratios in plasma extracellular vesicles are cell type-specific and are candidate biomarkers for inflammatory diseases. *Journal of Extracellular Vesicles*, *9*(1), 1764213. https://doi.org/10.1080/20013078.2020.1764213

Fujiwara, M., Kwok, S., Yano, H., & Pai, R. K. (2012). Arginase-1 is a more sensitive marker of hepatic differentiation than HepPar-1 and glypican-3 in fine-needle aspiration biopsies. *Cancer Cytopathol*, *120*(4), 230–237. https://doi.org/10.1002/cncy.21190

Gomes, D. E., & Witwer, K. W. (2022). L1CAM-associated extracellular vesicles: A systematic review of nomenclature, sources, separation, and characterization. *Journal of Extracellular Biology*, *1*(3), e35. https://doi.org/10.1002/jex2.35

Hoshino, A., Kim, H. S., Bojmar, L., Gyan, K. E., Cioffi, M., Hernandez, J., Zambirinis, C. P., Rodrigues, G., Molina, H., Heissel, S., Mark, M. T., Steiner, L., Benito-Martin, A., Lucotti, S., Di Giannatale, A., Offer, K., Nakajima, M., Williams, C., Nogués, L., … Lyden, D. (2020). Extracellular vesicle and particle biomarkers define multiple human cancers. *Cell*, *182*(4), 1044–1061. e1018. https://doi.org/10.1016/j.cell.2020.07.009

Huang, Y., Driedonks, T. A. P., Cheng, L., Rajapaksha, H., Routenberg, D. A., Nagaraj, R., Redding, J., Arab, T., Powell, B. H., Pletniková, O., Troncoso, J. C., Zheng, L., Hill, A. F., Mahairaki, V., & Witwer, K. W. (2022). Brain tissue-derived extracellular vesicles in Alzheimer's disease display altered key protein levels including cell type-specific markers. *Journal of Alzheimer's Disease*, *90*(3), 1057–1072. https://doi.org/10.3233/JAD-220322

Huang, Y., Driedonks, T. A. P., Cheng, L., Rajapaksha, H., Turchinovich, A., Routenberg, D. A., Nagaraj, R., Redding-Ochoa, J., Arab, T., Powell, B. H., Pletnikova, O., Troncoso, J. C., Zheng, L., Hill, A. F., Mahairaki, V., & Witwer, K. W. (2022). Relationships of APOE genotypes with small RNA and protein cargo of brain tissue extracellular vesicles from patients with late-stage AD. *Neurology Genetics*, *8*(6), e200026. https://doi.org/10.1212/NXG.0000000000200026

Hurwitz, S. N., Olcese, J. M., & Meckes, D. G. Jr. (2019). Extraction of extracellular vesicles from whole tissue. *Journal of Visualized Experiments*, 2019(144). https://doi.org/10.3791/59143

Li, D., Lai, W., Fan, D., & Fang, Q. (2021). Protein biomarkers in breast cancer-derived extracellular vesicles for use in liquid biopsies. *American Journal of Physiology-Cell Physiology*, *321*(5), C779–C797. https://doi.org/10.1152/ajpcell.00048.2021

Lim, C. Z. J., Natalia, A., Sundah, N. R., & Shao, H. (2020). Biomarker organization in circulating extracellular vesicles: New applications in detecting neurodegenerative diseases. *Advanced Biosystems*, *4*(12), e1900309. https://doi.org/10.1002/adbi.201900309

Mistlberger-Reiner, A., Sterneder, S., Reipert, S., Wolske, S., & Somoza, V. (2023). Extracellular vesicles and particles modulate proton secretion in a model of human parietal cells. *ACS Omega*, *8*(2), 2213–2226. https://doi.org/10.1021/acsomega.2c06442

Morris, K. V., & Witwer, K. W. (2022). The evolving paradigm of extracellular vesicles in intercellular signaling and delivery of therapeutic RNAs. *Molecular Therapy*, *30*(7), 2393–2394. https://doi.org/10.1016/j.ymthe.2022.05.015

Muth, D. C., McAlexander, M. A., Ostrenga, L. J., Pate, N. M., Izzi, J. M., Adams, R. J., Pate, K. A., Beck, S. E., Karim, B. O., & Witwer, K. W. (2015). Potential role of cervicovaginal extracellular particles in diagnosis of endometriosis. *BMC Veterinary Research*, *11*, 187. https://doi.org/10.1186/s12917-015-0513-7

Naujock, M., Speidel, A., Fischer, S., Kizner, V., Dorner-Ciossek, C., & Gillardon, F. (2020). Neuronal differentiation of induced pluripotent stem cells from schizophrenia patients in two-dimensional and in three-dimensional cultures reveals increased expression of the Kv4.2 subunit DPP6 that contributes to decreased neuronal activity. *Stem Cells and Development*, *29*(24), 1577–1587. https://doi.org/10.1089/scd.2020.0082

Newman, L. A., Muller, K., & Rowland, A. (2022). Circulating cell-specific extracellular vesicles as biomarkers for the diagnosis and monitoring of chronic liver diseases. *Cellular and Molecular Life Sciences*, *79*(5), 232. https://doi.org/10.1007/s00018-022-04256-8

Nikoobakht, M., Shamshiripour, P., Shahin, M., Bouzari, B., Razavi-Hashemi, M., Ahmadvand, D., & Akbarpour, M. (2021). A systematic update to circulating extracellular vesicles proteome; transcriptome and small RNA-ome as glioma diagnostic, prognostic and treatment-response biomarkers. *Cancer Treatment and Research Communications*, *30*, 100490. https://doi.org/10.1016/j.ctarc.2021.100490

Ohrfelt, A., Brinkmalm, A., Dumurgier, J., Brinkmalm, G., Hansson, O., Zetterberg, H., Bouaziz-Amar, E., Hugon, J., Paquet, C., & Blennow, K. (2016). The pre-synaptic vesicle protein synaptotagmin is a novel biomarker for Alzheimer's disease. *Alzheimers Research & Therapy*, *8*(1), 41. https://doi.org/10.1186/s13195-016-0208-8

Oliver, D., & Reddy, P. H. (2019). Dynamics of dynamin-related protein 1 in Alzheimer's disease and other neurodegenerative diseases. *Cells*, *8*(9), 961. https://doi.org/10.3390/cells8090961

Ostenfeld, M. S., Jensen, S. G., Jeppesen, D. K., Christensen, L. L., Thorsen, S. B., Stenvang, J., Hvam, M. L., Thomsen, A., Mouritzen, P., Rasmussen, M. H., Nielsen, H. J., Ørntoft, T. F., & Andersen, C. L. (2016). miRNA profiling of circulating EpCAM(+) extracellular vesicles: Promising biomarkers of colorectal cancer. *Journal of Extracellular Vesicles*, *5*, 31488. https://doi.org/10.3402/jev.v5.31488

Ramos-Zaldivar, H. M., Polakovicova, I., Salas-Huenuleo, E., Corvalan, A. H., Kogan, M. J., Yefi, C. P., & Andia, M. E. (2022). Extracellular vesicles through the blood-brain barrier: A review. *Fluids and Barriers of the Cns*, *19*(1). https://doi.org/10.1186/s12987-022-00359-3

Rhode, P., Mehdorn, M., Lyros, O., Kahlert, C., Kurth, T., Venus, T., Schierle, K., Estrela-Lopis, I., Jansen-Winkeln, B., Lordick, F., Gockel, I., & Thieme, R. (2021). Characterization of total RNA, CD44, FASN, and PTEN mRNAs from extracellular vesicles as biomarkers in gastric cancer patients. *Cancers (Basel)*, *13*(23), 5975. https://doi.org/10.3390/cancers13235975

Saint-Pol, J., Gosselet, F., Duban-Deweer, S., Pottiez, G., & Karamanos, Y. (2020). Targeting and crossing the blood-brain barrier with extracellular vesicles. *Cells*, *9*(4), 851. https://doi.org/10.3390/cells9040851

Saludas, L., Garbayo, E., Ruiz-Villalba, A., Hernandez, S., Vader, P., Prosper, F., & Blanco-Prieto, M. J. (2022). Isolation methods of large and small extracellular vesicles derived from cardiovascular progenitors: A comparative study. *European Journal of Pharmaceutics and Biopharmaceutics*, *170*, 187–196. https://doi.org/10.1016/j.ejpb.2021.12.012

Shetty, A. K., & Upadhya, R. (2021). Extracellular vesicles in health and disease. *Aging and Disease*, *12*(6), 1358–1362. https://doi.org/10.14336/AD.2021.0827

Thakur, A., Ke, X., Chen, Y. W., Motallebnejad, P., Zhang, K., Lian, Q., & Chen, H. J. (2022). The mini player with diverse functions: Extracellular vesicles in cell biology, disease, and therapeutics. *Protein Cell*, *13*(9), 631–654. https://doi.org/10.1007/s13238-021-00863-6

van Niel, G., Carter, D. R. F., Clayton, A., Lambert, D. W., Raposo, G., & Vader, P. (2022). Challenges and directions in studying cell-cell communication by extracellular vesicles. *Nature Reviews Molecular Cell Biology*, *23*(5), 369–382. https://doi.org/10.1038/s41580-022-00460-3

Willms, E., Cabanas, C., Mager, I., Wood, M. J. A., & Vader, P. (2018). Extracellular vesicle heterogeneity: Subpopulations, isolation techniques, and diverse functions in cancer progression. *Frontiers in Immunology*, *9*, 738. https://doi.org/10.3389/fimmu.2018.00738

Zhao, Z., Muth, D. C., Mulka, K., Liao, Z., Powell, B. H., Hancock, G. V., Metcalf Pate, K. A., & Witwer, K. W. (2020). miRNA profiling of primate cervicovaginal lavage and extracellular vesicles reveals miR-186-5p as a potential antiretroviral factor in macrophages. *FEBS Open Bio*, *10*(10), 2021–2039. https://doi.org/10.1002/2211-5463.12952

Zoltowska, K. M., Maesako, M., Lushnikova, I., Takeda, S., Keller, L. J., Skibo, G., Hyman, B. T., & Berezovska, O. (2017). Dynamic presenilin 1 and synaptotagmin 1 interaction modulates exocytosis and amyloid beta production. *Molecular Neurodegeneration*, *12*(1), 15. https://doi.org/10.1186/s13024-017-0159-y

SUPPORTING INFORMATION

Additional supporting information can be found online in the Supporting Information section at the end of this article.

How to cite this article: Abdelmohsen, K., Herman, A. B., Carr, A. E., Henry-Smith, C'. A., Rossi, M., Meng, Q., Yang, J.-H., Tsitsipatis, D., Bangura, A., Munk, R., Martindale, J. L., Nogueras-Ortiz, C. J., Hao, J., Gong, Y., Liu, Y., Cui, C.-Y., Hartnell, L. M., Price, N. L., Ferrucci, L., … Gorospe, M. (2023). Survey of organ-derived small extracellular vesicles and particles (sEVPs) to identify selective protein markers in mouse serum. *Journal of Extracellular Biology*, *2,* e106. https://doi.org/10.1002/jex2.106